Molecular Crystals and Liquid Crystals Science and Technology. Section A. Molecular Crystals and Liquid Crystals
Publication details, including instructions for authors and subscription information:
http://www.tandfonline.com/loi/gmcl19

Freedericksz Transitions in Nematic and Cholesteric Liquid Crystal Droplets: Determination of K_{24} Elastic Constant

S. Žumer [a], S. Kralj [a b] & J. Bezič [a]

[a] Physics Department, University of Ljubljana, Jadranska 19, 61000, Ljubljana, Yugoslavia

[b] J. Stefan Institute, University of Ljubljana, Jadranska 19, 61000, Ljubljana, Yugoslavia

Version of record first published: 24 Sep 2006.

To cite this article: S. Žumer , S. Kralj & J. Bezič (1992): Freedericksz Transitions in Nematic and Cholesteric Liquid Crystal Droplets: Determination of K_{24} Elastic Constant, Molecular Crystals and Liquid Crystals Science and Technology. Section A. Molecular Crystals and Liquid Crystals, 212:1, 163-172

To link to this article: http://dx.doi.org/10.1080/10587259208037256

Mol. Cryst. Liq. Cryst. 1992, Vol. 212, pp. 163–172
Reprints available directly from the publisher
Photocopying permitted by license only

Printed in the United States of America

FREEDERICKSZ TRANSITIONS IN NEMATIC AND CHOLESTERIC LIQUID CRYSTAL DROPLETS : DETERMINATION OF K_{24} ELASTIC CONSTANT

S. Žumer, S.Kralj*, and J.Bezič,
Physics Department and J. Stefan Institute*, University of Ljubljana
Jadranska 19, 61000 Ljubljana, Yugoslavia

(*Received April 15, 1991*)

ABSTRACT Field induced structural (Freedericksz) transitions in supramicron nematic and cholesteric liquid crystal droplets embedded in a solid matrix are theoretically analysed. Taking into account the elastic, surface, and field free energy contributions, the equilibrium structures and phase diagrams are obtained. The predicted strong dependence of the radial - axial structural transition on the value of the saddle splay elastic constant K_{24} is proposed to be used for the indirect determination of this constant.

Keywords: nematic, droplets, Freedericksz, elastic constants

INTRODUCTION

There is a constantly growing interest in spatially confined liquid crystals particularly after the appearance of liquid crystal shutters and displays based on the principle of electrically controlled light scattering exhibited by polymer dispersed liquid crystals (PDLC)[1-3]. These are dispersions of micron size liquid crystal droplets embedded in a solid polymer matrix. Usually droplets with a nearly uniform radius are formed during the polymerization process of the liquid crystal-prepolymer mixture[3]. The average droplet radius varies from the submicron region up to a hundred microns depending on the conditions during the formation process. Structures of such droplets which result from an interplay between elastic forces, external fields and surface interactions, can be completely characterized by a tensorial order parameter field. Here we limit our discussion to supramicron droplets where the variation of the orientational order parameter S is localized to relatively small regions (cores of the defects and surface layers[4]) which can be neglected or treated separately so that the structure is well characterized by the director field alone.

Since the first theoretical analysis of droplet structures[5] several experimental and theoretical studies have been devoted to supramicron nematic droplets[6-12]. The most common droplet director fields are bipolar[5-10] and concentric[9] for the tangential surface anchoring and radial[5,7] and

axial[7,10] structures for homeotropic anchoring. For materials with small twist elastic constants a reduction of the splay elastic free energy leads to twisted structures[9,11]. In droplets where anchoring is neither homeotropic or parallel, structures with lower symmetry appear[12]. Much less is known about cholesteric droplets. In the case of the tangential surface anchoring spherical structures with radial and diametrical defect lines[13-15] and planar structures with helical defect lines[14,16] are the most common.

In this paper we are going to discuss field induced transitons between some droplet structures. In the Section II we start with the free energy of a confined liquid crystal. In Section III the radial - axial transition is discussed in detail, particularly the possible determination of the K_{24} elastic constant. Section IV is devoted to the spherical - planar transition in a cholesteric droplet.

FREE ENERGY

To determine the stable structure of a chosen system usually the minimization of the free energy is used. We divide the corresponding free energy density in homogenous (f_o), elastic (f_e), interfacial (f_s) and field (f_f) part. The free energy density of an undeformed nematic or cholesteric phase f_o is usually described by a Landau expansion in terms of powers of the order parameter[17]. Within our approximation it is a temperature dependent parameter which will be used only in the estimation of the radii of defect cores.

The inhomogenous part of the free energy density of nematic or cholesteric liquid crystals is in a constant order parameter approach reduced to the Frank elastic free energy[17]

$$f_e(\vec{r})=\tfrac{1}{2}[K_{11}(\vec{\nabla}.\vec{n})^2+K_{22}(\vec{n}.\vec{\nabla}x\vec{n}+q)^2+K_{33}(\vec{n}x\vec{\nabla}x\vec{n})^2-K_{24}\vec{\nabla}.(\vec{n}(\vec{\nabla}.\vec{n})+\vec{n}x\vec{\nabla}x\vec{n})]. \quad (1)$$

K_{11}, K_{22}, K_{33} are the well known bulk Frank elastic constants and K_{24} the saddle-splay elastic constant corresponding to the surface elastic free energy term. q is the characteristic wave vector of the cholesteric structure. The K_{13} splay-bend term which includes second derivatives of the director field is omitted[18]. Further we assume a delta function interaction of the liquid crystal with the surrounding medium :

$$f_s(\vec{r}) = (1-(\vec{n}.\vec{e}_r)^2)\,\frac{W_o}{2}\,\delta(\vec{r}-\vec{R}) \quad (2)$$

characterized by the anchoring strength W_o[19] and the preferred anchoring

direction $\vec{e}_r$ on the droplet surface . The expression

$$f_f = -\frac{\mu_o}{2} \Delta\chi (\vec{H}.\vec{n})^2 \qquad (3)$$

describes the interaction with an external magnetic field $\vec{H}$, where $\Delta\chi$ is the difference between the principal values corresponding to the directions parallel and perpendicular to $\vec{n}$. It should be stressed that the effect of the electric field could be treated in a similar way, but in comparison to the magnetic field case it substantially varies over the droplet in most cases. Therefore a complete solution of the electric case can be obtained by solving the corresponding Maxwell equations simultaneously with the minimization of the free energy.

To find stable structures one must minimize the total free energy $F = \int (f_o+f_e+f_s+f_f)\, d^3\vec{r}$ for the particular case. This can be achieved either by a direct minimization[20] or by solving the corresponding Euler-Lagrange differential equations.

RADIAL-AXIAL TRANSITION IN NEMATIC DROPLETS: THE DETERMINATION OF K_{24}

This transition occurs in droplets where the confining surface induces homeotropic anchoring. The radial structure has a central point defect and a mostly radial director field (Fig.1a). In the central region of the axial structure the director field is predominantly axial but close to the surface it more or less satisfies the preferred direction (Fig.1b,c). To calculate these director fields we limit our discussion to cases without twist deformations, so the nematic director can be expressed in spherical coordinate system as

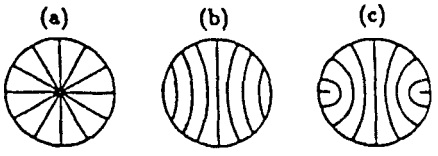

FIGURE 1 A shematic representation of the most common structures in nematic droplets with homeotropic anchoring: (a) radial, (b) axial without defects, and (c) axial with an equatorial line defect.

$$\vec{n} = -\sin\theta\, \vec{e}_\vartheta + \cos\theta\, \vec{e}_r, \qquad (4)$$

where $\vec{e}_r$ and $\vec{e}_\vartheta$ are unit vectors of the spherical coordinate system and θ the angle between $\vec{e}_r$ and $\vec{n}$. Introducing Eq. (4) into the free energy the Euler Lagrange equations are reduced to two equations for the scalar field $\theta(r,\vartheta)$.

The equation

$$(\sin^2\theta + \frac{K_{33}}{K_{11}}\cos^2\theta)(\frac{\partial^2\theta}{\partial\rho^2}\rho^2+2\frac{\partial\theta}{\partial\rho}\rho) + (\cos^2\theta + \frac{K_{33}}{K_{11}}\sin^2\theta)(\frac{\partial^2\theta}{\partial\vartheta^2}+\frac{\partial\theta}{\partial\vartheta}\mathrm{ctg}\vartheta) -$$

$$\frac{\sin2\theta}{2}(\mathrm{ctg}^2\vartheta\text{-}1) - (1+\frac{K_{33}}{K_{11}})\,\mathrm{ctg}\vartheta\,\sin^2\theta + \frac{(1-K_{33}/K_{11})}{2}\,[\,\sin2\theta(\rho^2(\frac{\partial\theta}{\partial\rho})^2+\rho\frac{\partial\theta}{\partial\rho}\mathrm{ctg}\vartheta -$$

$$(\frac{\partial\theta}{\partial\vartheta})^2 + \frac{\partial\theta}{\partial\vartheta} + 2\rho\frac{\partial^2\theta}{\partial\rho\partial\vartheta}) + 2\cos2\theta\frac{\partial\theta}{\partial\vartheta}\frac{\partial\theta}{\partial\rho}\rho\,] - (\frac{R}{\xi})^2\rho^2\frac{\sin(2(\theta\text{-}\vartheta))}{2} = 0 \qquad (5)$$

is valid in the droplet while on the surface we have the condition

$$\frac{\partial\theta}{\partial\rho}(\sin^2\theta+\frac{K_{33}}{K_{11}}\cos^2\theta) + \frac{\partial\theta}{\partial\vartheta}(1-\frac{K_{33}}{K_{11}})\sin\theta\cos\theta - \cos\theta\sin\theta(2-\frac{K_{33}}{K_{11}}) +$$

$$\mathrm{ctg}\vartheta\sin^2\theta + \frac{R}{d}\cos\theta\sin\theta + \frac{K_{24}}{K_{11}}(\sin2\theta - \mathrm{ctg}\vartheta\sin^2\theta) = 0\,. \qquad (6)$$

Here $\rho=r/R$, $\xi^{-1}=H\sqrt{\mu_o\Delta\chi/K_{11}}$ is the correlation length measuring the effect of the field[17] and $d = K_{11}/W_o$ is the extrapolation length[21] measuring the effect of anchoring. The equations are solved numerically.

Beside the radial solution (Fig.1a) two solutions with an axial director field were obtained: the axial structure without defect (Fig.1b) and the axial structure with a line defect in the equatorial plane (Fig.1c).

Stability regions of the three structures are for two different sets of elastic constants presented in Fig.2. The ratio $R/d=W_oR/K_{11}$ on the vertical coordinate axis measures the relative anchoring strength and the ratio $d/\xi=H\sqrt{\mu_o\Delta\chi K_{11}}/W_o$ on the horizontal coordinate axis measures the relative field strength. The radial structure is stable for strong anchorings and weak fields. In the zero field the structure has a completely radial director field, which with increasing external field progressively deforms and partially aligns along $\vec{H}$ but the defect stays at the droplet center (Fig.3a,b). A highly aligned radial structure (Fig.3b) which has all deformation

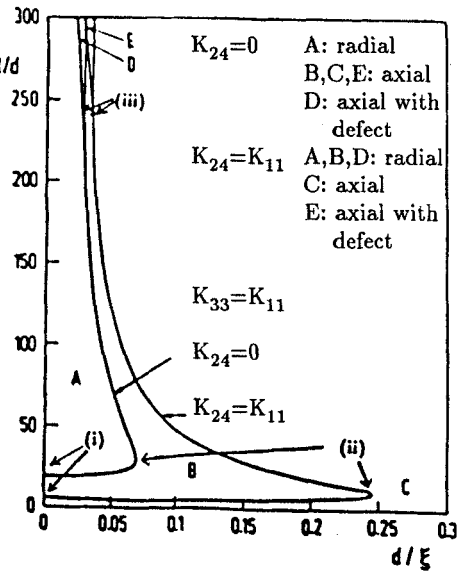

FIGURE 2 Phase stability diagram for two valuesof the elastic constant K_{24}.

concentrated near the equatorial plane is metastable.

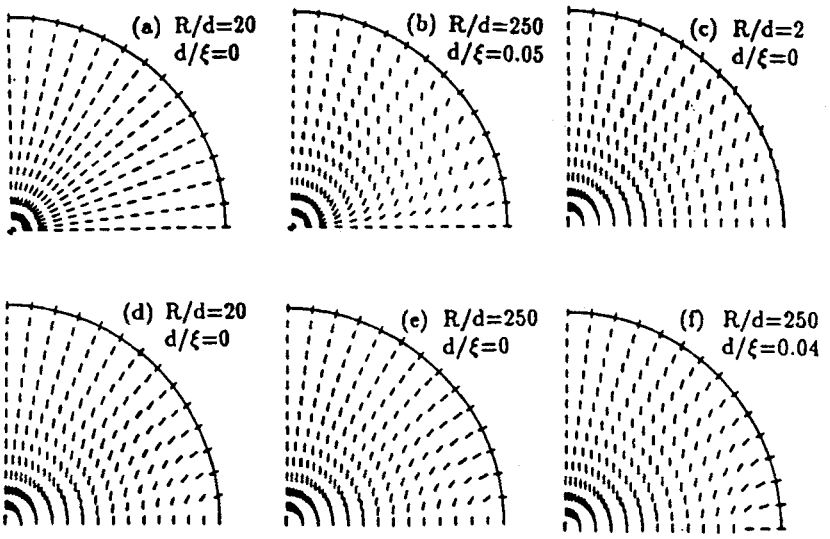

FIGURE 3 Director fields in spherical nematic liquid crystal droplets for different external fields and different homeotropic anchoring strengths: (a,b) radial, (c,d,e) axial without defects, and (f) axial with an equatorial line defect.

The axial structure without defects is stable in the weak anchoring regime or for any anchoring strength if the field is strong enough (Fig.3c,d,e). The degree of internal director alignment depends on the field and anchoring strength. (Compare Figs.3c,d,e ,. The axial structure with a defect line in the equatorial plane is stable only for strong anchoring in a very narrow region between radial and defectless axial stability regions (Fig.3f).

On the transition lines defined by the dependence of the transition radius R_t on the corresponding field H_t ($\propto \xi_t^{-1}$) there are three interesting points (Fig.2): (i) zero field radial-axial transition point, (ii) inversion point where the maximum transition field $H_{t\ max}$ is reached, and (iii) triple point where all three phases coexist.

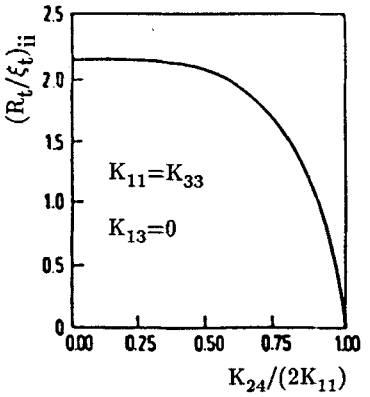

FIGURE 4 Dependence of the ratio R_t/ξ_t at the inversion point on the elastic constant K_{24}.

In this preliminary report we briefly discuss only the inversion point which strongy depends on the K_{24} elastic constant. An examination of the behavior of

the free energy shows[8] that for $K_{24}<2K_{11}$ the behavior of the ratio $(R_t/\xi_t)_{ii}$ at inversion point shown in Fig.4 would enable us to determine K_{24} if experimental data on $(R_t)_{ii}$ and $(\xi_t)_{ii}$ were available. Unfortunately the only known experiment was performed with electric field[22] and no reliable data on the internal field are available. Therefore only the existence of the inversion point can be used to conclude that $K_{24}<2K_{11}$ in the examined material.

SPHERICAL-PLANAR TRANSITION IN CHOLESTERIC DROPLETS

An undisturbed liquid crystal in the cholesteric phase forms a structure where nematic director field is homogeneous in any plane perpendicular to the helical axis. The direction of the field in these cholesteric planes progresively rotates when observed along the helical axis. The result of this rotation is a helical structure with a characteristic wave number q.

In confined cholesteric phases both nematic and helical ordering strongly depends on geometry and surface anchoring. We are limiting our discussion to the equilibrium structures in supramicron spherical droplets with parallel surface anchoring. Observations and theoretical predictions indicate that in such a case there are two types of cholesteric structures: those where cholesteric planes are deformed in concentric spheres - spherical structures[13,15] - and those where cholesteric planes do not deform - planar structures[14,16]. In both cases disclination lines are formed and several director fields are possible.

Spherical structures: In the equal elastic constant approximation $K_{11}=K_{22}=K_{33}$, $K_{24}\neq 0$ the minimization of the Frank free energy leads to the solution:

$$\vec{n}=\cos\Omega\,\vec{e}_{\vartheta}+\sin\Omega\,\vec{e}_{\varphi}, \quad \Omega=(s-1)\varphi+qr+\Omega_0 \tag{7}$$

where s can be 1, 3/2, 2 and Ω_0 is an arbitrary constant. (In this case the director field in the droplet is everywhere normal to the corresponding radius vector.) Taking into account the escape of the director field into the third dimension which can occur within the cores of line defects with s=1 or 2, one can show that the corresponding structures have lower free energy than the structure with an s=3/2 disclination line. Therefore we are going to consider only structures with s=1 and 2.

i) *Spherical structure with a diametrical defect.* The field lines on a concentric sphere corresponding to the chosen radius form a characteristic pattern. By

changing the radius the pattern continously performs a periodic transformation from a bipolar one via twisted bipolar to a concentric one and back (See Fig.5a.). Along the diametrical symmetry axis there is a line defect with strength 1.

ii) *Spherical structure with a radial defect.* Here the director field on each concentric sphere has the same pattern but the field lines are rotated from sphere to sphere (See Fig.5b). There is a line defect with s=2 parallel to the symmetry axis along one half of the diameter (radial defect line).

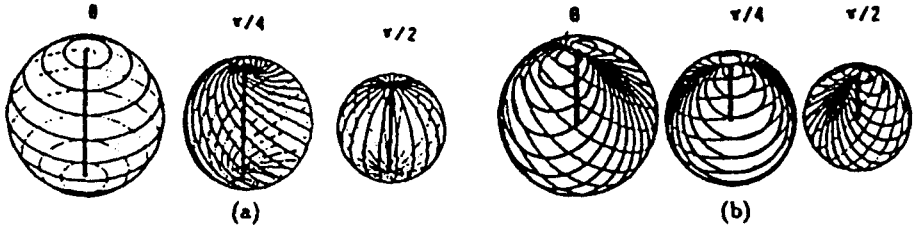

FIGURE 5 Spherical structures with (a) a diametrical defect line and (b) a radial defect line. Director field lines on concentric surfaces corresponding to $qr+\Omega_0=0$, $\pi/4$, $\pi/2$ are presented by thin lines and line defects by thick lines.

Using our solutions Eqs.(7) for the free energy density reduces to the case where $K_{11}=K_{22}=K_{33}$, $K_{24}=0$ and $W_0\to\infty$. The dependence of the free energy on the droplet radius is calculated (Fig.7). The core of the defect was assumed to be in the isotropic phase. The radius of this core was obtained by comparing the Landau free energy density of the undeformed cholesteric phase f_0 and the deformation free energy density (Eq.(1)). For a typical liquid crystal the radius r_1 of the core of a defect line with s=1 is about 20nm at 1K above the transition point.

Planar structure: Here the director field is everywhere planar. Similary as in the unbound cholesteric phase a helical axis perpedicular to the director field can be introduced. Along this axis the planar director field which has the same pattern in each plane progressively rotates. The planar field is constrained by the parallel surface anchoring. There are two simple cholesteric orderings:

(i) *planar monopolar structure,* where director fields are circles with one common point (defect) lying on the confining sphere (Fig.6a). On the droplet surface all these points form a helical disclination line with the strength 2 and pitch equal to $2\pi/q$.

(ii) *planar bipolar structure*[14,16], where director field in each plane is bipolar with two point defects on the confining sphere (Fig.6b). On the droplet

surface these points form two helical disclination lines with the strength 1 and pitch equal to $2\pi/q$.

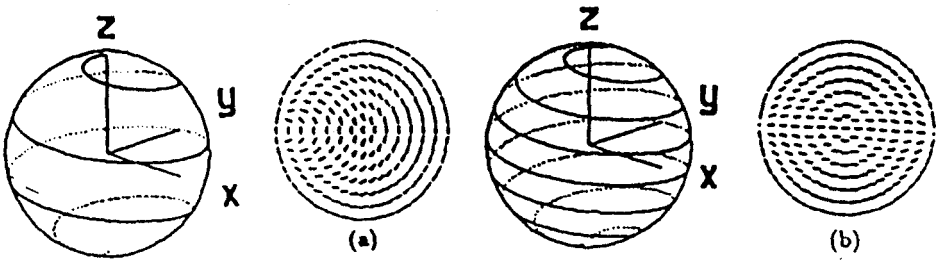

FIGURE 6 Helical disclination lines and director fields in planes perpendicular to z axis: (a) planar monopolar structure and (b) planar bipolar structure.

The elastic free energies of both structures as functions of the droplet radius are presented in Fig.7. Singular contributions of defect lines are again avoided by introducing the appropriate isotropic cores as for spherical structures. The resulting free energy is in all four cases proportional to $R\ln(R/r_1)$. Everywhere the planar bipolar structure has lower free energy than the planar monopolar structure. Comparing planar and spherical structures, one can conclude that in our approximation the spherical structure with the diametrical defect is the most stable one. By introducing different elastic constants, retaining the surface elastic terms in the Frank expression for elastic energy, and taking into account the possible escape of the director field in the cores of line disclinations, the relative stability of the structures certainly changes, but this is beyond the scope of this preliminary discussion.

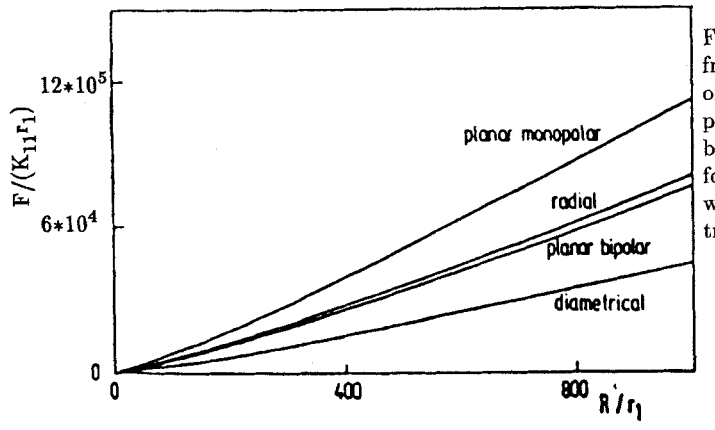

FIGURE 7 Zero field free energy dependence on the droplet radius for planar, monopolar and bipolar structures, and for spherical structures with radial and diametrical defect line.

According to the above discussion a transition from a spherical to planar structure can not be induced by a temperature change, but it can be caused by

an external electric (or magnetic) field if the liquid crystal material has negative dielectric (or diamagnetic) anisotropy[14]. For the transition of the spherical structure with a diametrical defect to the planar bipolar structure the dependence of the critical field E_C (or H_C) on the droplet radius is shown in Fig.8. In our simplified calculation we assumed that the director field in a spherical structure is not deformed by the presence of an external field and that the diametrical defect line is parallel to the field. Therefore the field part of the free energy is roughly proportional to R^3 and the corresponding critical field to $\sqrt{\ln R}/R$. The minor oscilations which are caused by more or less favourable director orientations in additional cholesteric spheric layers which contribute to the free energy of the droplets with larger radii, slowly vanishes as qR becomes much larger than 1.

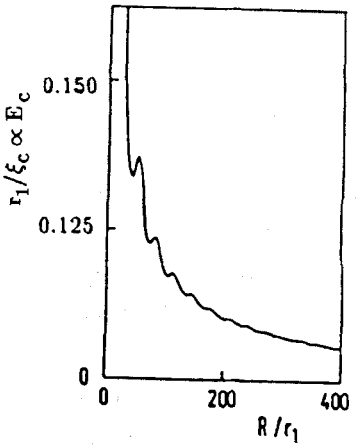

FIGURE 8 Dependence of the critical field $E_c \propto \xi_c^{-1}$ (ξ_c-the corresponding correlation length) on the droplet radius.

Taking typical values $K_{11}=5\text{x}10^{-12}$N, $\Delta\epsilon$=-4.5, r_1=20nm the transition in a droplet with R=7.5μm at qR=40 occurs at $E_C=4.10^5$V/m which is close to the transition field observed by Yang and Crooker[14] for the droplets of the mentioned size. But it should be stressed that the observed transition is not immediate and there are some intermediate structures which can not be explained within our simple model.

CONCLUSIONS

The complete phase diagram for a nematic droplet with a homeotropic surface anchoring was determined. The study of the dependence of the radial-axial Freedericksz transition on the sadle splay elastic constant K_{24} have shown that this constant can be determined from the experimentally obtained values of the transition field and radius corresponding to the inversion point.

The preliminary study of the stable sperical and planar structures of a cholesteric droplet in the external field was used to estimate the corresponding critical transition field. To explain the available experimental data[14] a more detailed study of the escaped and field deformed structures must be

performed.

REFERENCES

1. J.W.Doane, N.A.Vaz, B.G.Wu, S.Žumer, Appl.Phys.Lett.48, 269 (1986).
2. J.Fergason, SID (Society for Information Display), Int. Symposium Digest of Tehnical Papers 16, 68 (1985).
3. J.W.Doane, A.Golemme, J.L.West, J.B.Whitehead, B.G.Wu, Mol.Cryst.Liq.Cryst. 165, 511 (1988).
4. S.Kralj, S.Žumer, D.W.Allender, Phys.Rev.A 43, 2943 (1991).
5. E.Dubois-Violette, O.Parodi, J.Phys.C4 30, 57 (1969).
6. G.E.Volovik, O.D.Lavrentovich, Zh.Eksp.Teor.Fiz. 85, 1997 (1983); Sov.Phys.JETP 58, 1159 (1983).
7. S.Žumer, J.W.Doane, Phys.Rev.34, 3373 (1986).
8. S.Kralj, S.Žumer, to be published.
9. P.Drzaic, Mol.Cryst.Liq.Cryst. 154, 289 (1988).
10. S.Candau, P.LeRoy, F. Debeauvais, Mol.Cryst.Liq.Cryst. 23, 283 (1973).
11. R.D.Williams, J.Phys.A:Math.Gen.19, 3211 (1986).
12. M.V.Kurik, O.D.Lavrentovich, E.M.Terentev, Usp.Fiz.Nauk.154, 381 (1988).
13. Y. Bouligand, F.Livolant, J.Phys.(Paris) 45, 1899 (1984).
14. D.K.Yang, P.P.Crooker, Liq.Cryst. 9, 245 (1991).
15. J.Bezič, S.Žumer, to be published.
16. J.R.Quigley, W.J.Benton, Mol.Cryst.Liq.Cryst. 42, 43 (1977).
17. G.Vertogen, W.H. de Jeu, Thermotropic Liquid Crystals (Springer Verlag, Heidelberg, 1988).
18. A.Strigazzi, Il Nuovo Cimento 10D, 1335 (1988).
19. H.Yokoyama, S.Kobayashi, H.Kamei, J.Appl.Phys. 6, 4501 (1986).
20. I.Vilfan, M.Vilfan, S.Žumer, Phys.Rev.A, 4724 (1990).
21. De Gennes, The Physics of Liquid Crystals (Clarendon, 1974).
22. J.H.Erdmann, S.Žumer, J.W.Doane, Phys.Rev.Lett. 64, 19 (1990).